Ablation Mass Loss of an Electric Solid Propellant in a Pulsed Plasma Thruster

IEPC-2017-376

Presented at the 35th International Electric Propulsion Conference
Georgia Institute of Technology • Atlanta, Georgia • USA
October 8 – 12, 2017

Matthew S. Glascock[1]
Missouri University of Science and Technology, Rolla, Missouri, 65409 USA

and

Joshua L. Rovey.[2]
University of Illinois Urbana-Champaign, Urbana, Illinois, 61801 USA

Electric solid propellants are solid rocket propellants that are only ignited and burned when electric power is applied. This type of propellant may be used in an electric propulsion system, specifically a pulsed plasma thruster. In this work, the ablation mass loss of an electric solid propellant is investigated. A test article is utilized wherein an arc discharge of 10 Joules per pulse is created in a tube of propellant. Measurements of the mass loss over many discharges are presented for both the electric solid propellant and Teflon, the typical propellant for a pulsed plasma thruster. Results indicate an average specific ablation of 1.99 μg/J for Teflon and 2.87 μg/J for the electric solid propellant. Additionally, the equivalent initial resistance and inductance of the arc discharge are estimated using a circuit model. The resistance values are similar for the two propellants and are about 150 mΩ. Inductance values are estimated to be ~760 nH for Teflon and ~450 nH for the electric solid propellant.

Nomenclature

V_0	= initial capacitor voltage
C	= capacitance of main capacitor
$I(t)$	= current measured through arc discharge
$L(t)$	= time-variable inductance
$R(t)$	= time-variable resistance
$V(t)$	= voltage across the capacitor
L_0	= inductance of circuit model at time zero
R_0	= resistance of circuit model at time zero
$Q(t)$	= time-variable charge stored on capacitor
Q_0	= charge stored on capacitor at time zero
ω	= frequency of undamped oscillatory current solution
P	= oscillatory period of current solution
S	= sum of squared residuals
r_i	= residual value at time t_i
t_i	= discrete values of time for measured current waveform
I_{EXP}	= value of measured current at time t_i
I	= value of current solution at time t_i

[1] Graduate Research Assistant, Mechanical and Aerospace Engineering, msgdm3@mst.edu.
[2] Associate Professor of Aerospace Engineering, 317 Talbot Lab, 104 S. Wright St., rovey@illinois.edu.

I. Introduction

ELECTRIC solid propellants (ESP's) are an emerging topic of research with major implications in the field of propulsion from the micro to macro scale[1-3]. These propellants offer exciting capabilities for controlling solid chemical rocket motors previously unheard of for typical energetic materials. When electric power at the proper current and voltage levels is applied to an ESP, the solid propellant ignites and continues to exothermically decompose until that power is removed. This process can be repeated until the solid propellant is entirely consumed. Further, the burn rate of the propellant can be throttled by altering the electrical power applied. This method of operation is not possible with traditional solid rocket propellants and energetics, and greatly expands the potential applications for solid rocket motors that are fit with an ESP. Additionally, ESPs are insensitive to accidental ignition by spark, impact or even open flame. This is a huge advantage over most energetics in safety considerations and ease of use.

The development of ESPs began in the mid-late 90's with the investigation of a "green" automobile air bag inflator propellant (ABIP). This ammonium nitrate based material quickly garnered attention from the U.S. Air Force for other applications, including a patented formulation for rocket propulsion application. Soon after, the first controlled extinguishable solid propellants were developed, the first of which was referred to as "ASPEN." This development process began adding ingredients to the ammonium nitrate based propellant to lower the melting point and increase the electrical conductivity during chemical combustion. Performance metrics of the ASPEN propellant were comparable to typical marks for solid rocket motors, but experienced major problems with initial ignition. Addressing these problems led to the development of a more advanced formula to achieve higher specific impulse and conductivity of the propellant. This higher performance electric propellant (HIPEP) is a hydroxyl ammonium nitrate (HAN) based energetic material. In this formulation, the ionic liquid oxidizer HAN exhibits a pyroelectric behavior; the application of electric power to this material incites the creation of nitric acid, triggering ignition of the formulation. ESPs have also been tested for application in electric propulsion. The aforementioned ABIP was tested as alternative fuel/propellant for the ablation fed pulsed plasma thruster. In Aerojet's Modular Test Unit (MTU), three formulations showed impulse bit marks in the range of 50-80% of the traditional Teflon propellant[3].

The Pulsed Plasma Thruster[4] (PPT) has been in service as an in-space electric propulsion technology since 1968. Advantages include higher exhaust velocities than chemical thrusters with an inert, solid propellant on spacecraft that have the electric power already available. PPT's typically fulfill secondary propulsion needs such as station-keeping[5-7] and attitude control[8,9]. Burton and Turchi[4] stated PPT's may be classified in one of two geometries: rectangular and coaxial. The coaxial PPT, like that of the University of Illinois PPT-3 and 4[10,11], begins with a central and downstream electrode, often with a conical shape between the two. The central electrode is usually a solid (rod) electrode while the downstream is ring-shaped, and either can be selected as the positively charged electrode (anode). The igniter plug is always located in the cathode, regardless of whether it is the central or downstream electrode. Solid propellant fills the space between the electrodes, usually in the form of a tube or rods. A small amount of this propellant, usually polytetrafluoroethylene (PTFE or Teflon) is ablated during the main capacitor arc discharge and accelerated to high velocity. The mechanism for this acceleration is predominantly electrothermal in coaxial PPT's, i.e. the high temperatures inherent to an arc discharge provide sufficient energy to the particles in the gas to provide a high exit velocity. The process of ablation is essential to the operation of the coaxial PPT, and a number of studies in the ablation of PTFE have been previously conducted in the literature[12-17]. One such study by Seeger et al. used a "small scale test device" similar to that of a high voltage circuit breaker using PTFE[18]. The design of the test article in this work is based on the small scale device in Seeger's work.

In this work, a small scale test device similar to a high voltage circuit breaker is tested with both PTFE and the HAN-based HIPEP. In each propellant testing case, the ablated mass per pulse is measured, and the discharge current waveform is measured and then analytically modeled. Comparison of the measured ablation mass bit and the estimated electrical characteristics allow for insights into the behavior the HIPEP in a pulsed plasma thruster.

II. Experimental

A. Vacuum Facility and Mass Balance

The space and high-altitude vacuum facility in the Aerospace Plasma Lab at Missouri S&T was used to conduct the tests in this work. The facility has a test area of about 6 ft (1.8 m) in diameter and 10 ft (3 m) in length. Four 89 cm diameter oil vapor diffusion pumps are the primary vacuum pumps and are backed by a Tokuda KP-7500BG rotary-vane and Edwards EH 4200 roots-blower pumps. This pump setup is diagramed in Figure 1. The diffusion

pumps are operated independently and with a single pump running (as was done during this work) the nominal base pressure is 3×10^{-5} Torr.

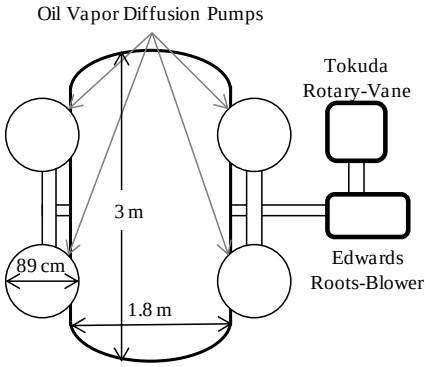

Figure 1: Space and high altitude vacuum facility at Missouri S&T.

For mass-loss measurements, a Sartorius QUINTIX125D-1S dual range semi-micro balance was used to measure the mass of propellant samples before and after testing. In the selected range, this balance has a capacity of 60 g and a readability of 0.01 mg. The factory reported repeatability of the balance is 0.02 mg.

B. High Performance Electric Propellant

The ESP is a HAN-based solution solid manufactured using benign processes and "green" ingredients, mixed in standard chemical glassware and cured at room temperature (35°C/95°F). It has a chemical composition of HAN oxidizer (an inorganic ionic liquid) and polyvinyl alcohol (PVA) fuel binder, which make up 95% of the propellant. The ESP is initially a liquid and poured into a mould. It is then cured to form a soft solid with the appearance and texture of a soft pencil eraser. There are some key differences between the ESP and traditional Teflon (PTFE) PPT propellant. PTFE is a fluorocarbon solid, while the ESP is a soft-solid mixture with composition given in Table I. In a typical PPT, the PTFE is an electrical insulator between the electrodes. The conductivity of the ESP in this work is comparable to "highly conductive" ionic liquids which have been selected as candidates for use in dye-sensitized solar cells[19]. With the ESP propellant the pulsed electric current could potentially be conducted through the ESP, initiating thermoelectric decomposition and creation of intermediates in the propellant. With PTFE an arc discharge is created near the surface of the solid PTFE, ablating the propellant via heat transfer. It is currently unclear how these propellant differences affect the operation and performance of a PPT using the ESP as a propellant.

Table I. Chemical composition of the High Performance Electric Propellant.

Chemical Name	Chemical Formula	Percentage by mass	Molecular Mass, g/mol
Hydroxyl Ammonium Nitrate (HAN)	$(NH_3OH)^+ NO_3^-$	75%	96
Polyvinyl Alcohol (PVA)	$CH_2CH(OH)$	20%	44
Ammonium Nitrate (AN)	NH_4NO_3	5%	80

C. Test Article

For the proposed study, a small scale coaxial geometry pulsed plasma discharge chamber has been designed and built as the test article for an ablation mass study. Figure 2 details the geometry of the test article assembly. A stainless steel rod serves as the anode (positive) and a graphite ring serves as the cathode (ground). The anode is kept isolated electrically from the aluminum housing by a PTFE sleeve. The propellant tube sample is shown in red (HIPEP) and

has a length of 0.5 in (12.7 mm) and diameter 0.25 in (6.35 mm). Because HIPEP is conductive, the propellant is isolated electrically from the two electrodes by thin PTFE washers with inner diameter ~7 mm, and from the aluminum housing by a PTFE sleeve. The washers remain during PTFE testing to keep electrode spacing consistent between propellant samples. The assembly is easily deconstructed via the threaded pipe fitting housing for the anode, allowing retrieval of the sample. On the downstream end, a vented hex head bolt serves to hold the assembly in place and allow the ablated propellant plume to exhaust.

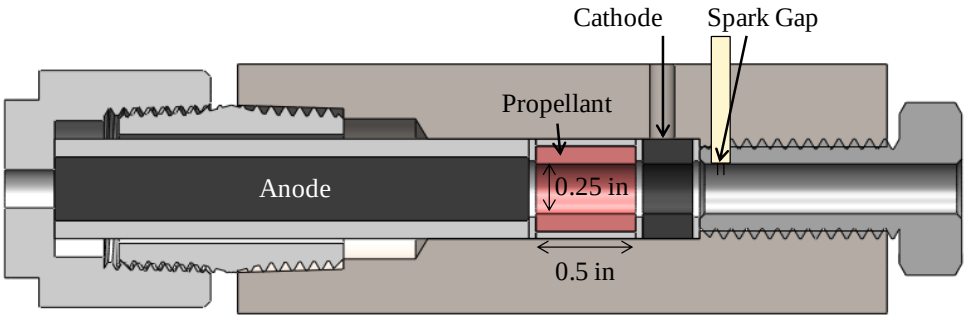

Figure 2: Diagram of the coaxial pulsed plasma discharge chamber test article.

The test article and the capacitor are inside the vacuum test facility. It is intended that the arc discharge occurs inside the tube of propellant between the anode and cathode. However, because the test article is at vacuum, the capacitor can be charged to a large voltage (1-5 kV) across the anode/cathode without initiating a Paschen breakdown. Thus, the arc discharge breakdown is initiated by a small spark gap featuring two tungsten wires cemented in a two-bore alumina tube with ~2 mm exposed tips. The wire tips are located in the exhaust channel just downstream of the cathode as shown in Figure 2. A capacitor discharge ignition (CDI) circuit creates a small spark across the tungsten wire tips, introducing a number of electrons into the cylindrical volume inside the tube of propellant. These charge carriers allow the flow of current to begin between the electrodes.

D. Electrical Setup

The electrical setup for the experiment is similar to that of a laboratory bench-top pulsed plasma thruster setup, and is diagramed in Figure 3. A high voltage power supply is set to the desired discharge voltage, V_0, and is connected to earth ground. The power supply unit is a Glassman HV FJ05R24 model with a maximum DC voltage output of 5 kV and current output of 24 mA. This supply charges the main capacitor with capacitance C through a 500 Ω high power charging resistor, which also serves to prevent current from back flowing into the high voltage supply. A single CSI Technologies capacitor rated up to 4 kV DC and measured to have a capacitance of 4.92 µF stores this discharge energy (up to ~40 J).

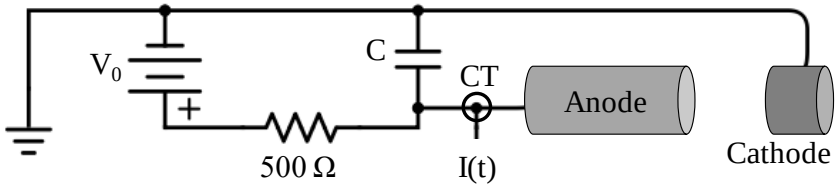

Figure 3: Circuit diagram for the pulsed plasma discharge chamber.

Not shown in the circuit diagram is the CDI spark gap circuit. The device used is an off-the-shelf unit with a capacitance of 0.47 µF and an output voltage of 30 kV. The energy stored in the unit, about 40 mJ, is small relative to the main capacitor. During each discharge, a pulse current transformer (CT) measures the current, *I(t)* through the anode side of the circuit.

III. LCR Circuit Model

Pulsed accelerators with thin arc current layers can be theoretically idealized as simple switched inductance-capacitance-resistance (LCR) series circuit[20]. Consider the circuit diagramed in Figure 4. A capacitance C is initially

charged to some voltage V_0. At time zero, the capacitance is switched across a time-variable inductance $L(t)$ and resistance $R(t)$. The initial inductance is determined both by circuit geometry and the inherent inductance of the capacitor. Initial resistance is a result of the external circuit resistance as well as a portion attributed to the arc discharge. Once the discharge is created, current $I(t)$ flows through the circuit as the voltage, $V(t)$, dissipates from the capacitor.

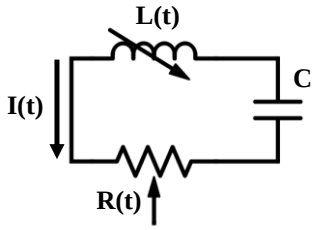

Figure 4: Ideal inductance-capacitance-resistance series circuit.

Examination of Maxwell's equation ($\boldsymbol{\nabla} \times \boldsymbol{E}$) around the circuit yields the differential Equation (1) for voltage and current in the single variable of time. Closer examination of this current-voltage characteristic equation yields the electrical efficiency of a pulsed accelerator[20].

$$V(t) = I(t)R(t) + \frac{d}{dt}\big(L(t)I(t)\big) = IR + L\frac{dI}{dt} + I\frac{dL}{dt} \tag{1}$$

At time zero, the initial inductance L_0 and resistance R_0 are fixed values. Thus, a coaxial arc discharge can be thought of as a simple LCR circuit with fixed elements L_0, C, and R_0. If we consider now the time-varying charge stored on the capacitor, $Q(t)$, where $V(t) = Q(t)/C$, Equation (1) can be rewritten as a differential Equation (2) in terms of $Q(t)$; note that $I(t) = -dQ/dt$. The solution of Equation (2) has two forms for the initial conditions $Q_0 = V_0C$ and $I_0 = 0$, the overdamped form and the underdamped oscillatory form.

$$L_0\frac{d^2Q}{dt^2} + R_0\frac{dQ}{dt} + \frac{Q}{C} = 0 \tag{2}$$

For practical values of initial inductance, resistance and capacitance, the solution of the differential equation takes the underdamped oscillatory form. This solution in $Q(t)$ can be rewritten in terms of the current $I(t)$ as Equation (3) below.

$$I(t) = -\frac{dQ}{dt} = \frac{V_0}{\omega L_0}\, e^{-\frac{R_0 t}{2L_0}} \sin(\omega t)$$

Where

$$\omega = \left(\frac{1}{L_0 C} - \frac{R_0^2}{4L_0}\right)^{1/2} \tag{3}$$

In this work, Equation (3) will be matched to the measured current waveform for a fixed V_0 test case. This is achieved by first matching the period of the sine function, $P = 2\pi/\omega$, to the numerically determined oscillatory period of the measured waveform from the test circuit. The period P is largely dominated by the value of L_0 such that we can assume R_0 is negligible in the period matching calculation and use $P = 2\pi(L_0C)^{1/2}$ to determine a value of L_0. The amplitude of the model prediction is determined largely by the value of R_0. With a fixed value of L_0, the resistance value can then be picked such that the model predicted values of I(t) best fit the measured current waveform in a least squares sense. That is, R_0 is iterated until S, the sum of residuals squared in Equation (4) is minimized.

$$S = \sum_{all\ i} r_i^2 = \sum_{i=0}^{n}\big(I_{EXP}(t_i) - I(t_i)\big)^2 \tag{4}$$

In Equation (4), $I_{EXP}(t)$ is the experimentally measured current waveform, $I(t)$ is the current predicted by the LCR circuit model. The residual r_i is the difference between these values for all discrete values of time, t_i, that the current is measured by the oscilloscope.

IV. Results and Discussion

A. Discharge Current

As detailed in the electrical setup, the current through the anode portion of the test article circuit is measured using a high current transformer for each discharge of the capacitor. The variance in this current waveform is less than 5% peak value from pulse to pulse at each selected voltage. Thus, for a single voltage an LCR circuit model current is fit to a representative current measurement to estimate a resistance value for the complete circuit. Figure 5 shows the experimental data and the LCR model current waveform side by side with the calculated circuit resistance and inductance for both PTFE and HIPEP at an initial voltage of 2000 V.

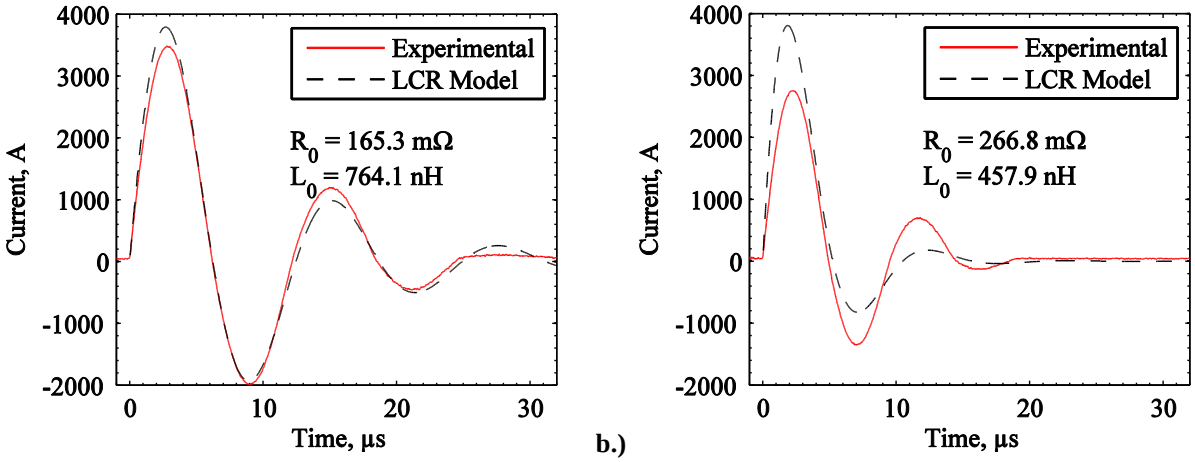

Figure 5: Circuit model current fit for a.) PTFE discharge and b.) HIPEP discharge at 2000 V.

The circuit model current best fits the experimental data for PTFE with R_0 = 165.3 mΩ and L_0 = 764.1 nH. Of importance to note is that the estimated resistance and inductance in the LCR model are equivalent values for the *entire* circuit. Both quantities are the sum of contributions from three primary sources: the capacitor, the electrodes and the plasma[21]. From the manufacturer, the typical inductance for the main capacitor is in the range of 100-200 nH. At a frequency of 100 kHz, the resistance of the capacitor is estimated to be in the 10-50 mΩ range. At room temperatures, the resistivity of stainless steel is ~7×10^{-7} Ω-m and the skin depth of 1.3 mm which provides an estimate of 1.2 mΩ for the resistance of the anode, and about the same for the graphite cathode. Thus, the resistance of the plasma is estimated to be on the order of 100 mΩ and the inductance in the range of 500-700 nH for the PTFE arc discharge. By integrating the measured instantaneous power through the circuit, $P = I_{EXP}(t)^2 R_0$, for PTFE it was found that 8.94 J was dissipated, which is ~91% of the 9.84 J stored on the capacitor at the initial voltage of 2000 V.

For HIPEP, the model best fits with R_0 = 266.8 mΩ and L_0 = 457.9 nH. These values are perhaps unexpected when compared with that of the PTFE model. One would expect that with a conductive propellant, the resistance of the circuit (and thus the plasma, as the circuit components remain the same) would decrease relative to that of an insulating propellant. However, this resistance is based on the chemical species present in the ablated gas that forms the plasma. For PTFE, the species are limited to Carbon and Fluorine atoms; for HIPEP, the species could be that of the equilibrium reaction products, reaction intermediates, water vapor or even raw propellant compounds. This makes the electrical behavior of the plasma difficult to predict. A significant change in inductance is also counterintuitive, as the geometry of the test article and its circuit was not changed between the two propellants. Again, the conductivity of HIPEP may be changing the parameters of the actual circuit, as now there exists a (floating) conductor in the space between the high voltage electrodes. Note however that the circuit model does not fit as well for HIPEP as it did for PTFE. During testing, an interesting phenomenon was noted. When using HIPEP, the voltage across the capacitor (as measured by the high voltage supply) would not decrease to zero during the discharge, possibly indicating that the stored energy on the main capacitor was unable to fully dissipate during the arc discharge. Indeed, integration of the measured current-squared, $P = I_{EXP}(t)^2 R_0$, dissipated through the resistance indicates that only 6.39 J, or 65% of the stored energy was dissipated. In light of this observation, a model "correction" of reducing the initial voltage on the main capacitor was introduced into the model for HIPEP. Figure 6 shows this adjusted circuit model for HIPEP.

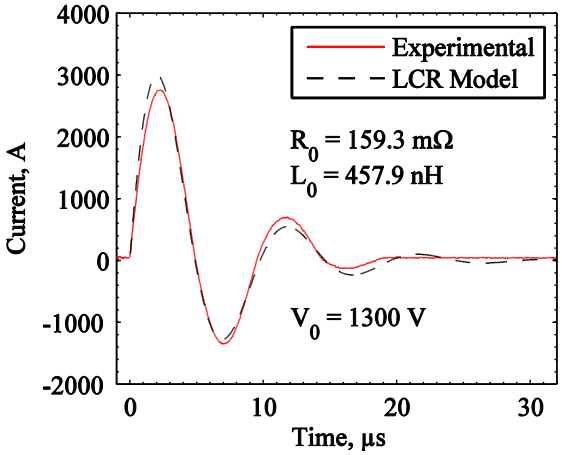

Figure 6: Circuit model fit for HIPEP discharge with a reduced initial voltage value.

In Figure 6 a voltage of 1300 V was used to account for the lack of complete energy dissipation from the capacitor. With this voltage, the model best fits experimental data with R_0 = 159.3 mΩ and L_0 = 457.9 nH. The small reduction in the resistance of the circuit relative to PTFE was originally expected when using the conductive HIPEP. Integration of the power dissipated yields a value of 3.82 J dissipated, which is only 39% of the stored energy of the capacitor. The exact cause of this phenomenon is unknown. It is possible it was due to an extinguishment of the arc discharge prematurely which could be caused by a large, rapid change in local pressure in the test article. Further, it is possible that some of the discharge energy is conducted through the propellant, though one would expect this current to also be measured by the transformer. Obviously, the phenomenon warrants further investigation beyond the scope of this work.

B. Ablation Mass Loss

At the selected voltage, three samples of each propellant were tested and the mass loss measured. Prior to testing the PTFE samples were put through a "burn-in" phase where the sample was brought to vacuum for a at least one hour and then the capacitor pulsed through the sample 15-20 times. This allowed both off-gassing of any absorbed moisture in the sample as well as burning off of any surface impurities that could interfere with mass measurements. After burn-in, the initial mass was measured to an accuracy of 0.01 mg and recorded. During testing, the discharge voltage was kept constant for a recorded number of pulses of the test article. The final mass was then recorded immediately after testing and pressurizing the vacuum facility. The mass loss is, of course, the difference in these two values. Table II details these values as well as calculated values for the change in mass per-pulse and per-energy stored on the main capacitor.

Table II: Ablation mass loss measurements for PTFE and HIPEP.

Propellant	Voltage, V	Mass Loss, mg	Pulses	Δm/Pulse, μg	Δm/Energy, μg/J
PTFE	2000	4.52	200	22.60	2.26
		2.95	150	19.67	1.97
		2.89	175	16.51	1.65
HIPEP	2000	24.28	75	323.73	32.37
		37.60	125	300.80	30.08
		40.36	130	310.46	31.05

For the PTFE measurements, an average change in mass per-pulse of 19.6 μg was measured. For the discharge energy of 9.84 J, this is a mass-per-energy of 1.99 μg. Burton and Turchi[4] reported similar values in the range of 1.5-10 μg/J for a number of PPT's, both coaxial and rectangular.

A previous investigation reported an ablation mass-per-energy of 5.4 µg/J for HIPEP[22-24]. In this work, the average mass-per-energy was measured to be 31.7 µg/J. However, it was expected that these numbers are inflated by the moisture content of the HIPEP, which does not go through a burn-in process like that of the PTFE in order to minimize the exposure of the samples to moisture vapor in the air. Thus, the measured mass loss value may contain the mass lost due to the evaporation of water absorbed in the material in addition to the mass ablated for each pulse. As such, further investigation into this behavior, specifically the contribution of volatile absorbed water to the mass loss, was conducted.

C. HIPEP Water Content

The primary constituent of HIPEP, HAN, is known to be very hygroscopic. Raw HIPEP samples rapidly absorb moisture from the atmosphere if left exposed to a humid environment, reducing entirely to a liquid if left for a long period of time. As such, an investigation of the moisture absorption rate of the material was conducted shortly after removal from vacuum. Using the high accuracy semi-micro balance, the mass of a sample of HIPEP was recorded over a period of 20 minutes at room temperature of about 296 K, 101 kPa pressure, and a relative humidity of ~50%. These data are shown in Figure 7, along with a linear data fit. The linear data fit indicates a moisture absorption rate of about 0.75 mg/min. If the time between venting of the vacuum facility and the mass measurement of the sample is recorded, the mass of the sample in vacuum (i.e. without moisture) can be estimated from the absorption rate, assuming the same linear relationship is valid from the time the facility is vented to atmosphere and the sample is extracted and weighed.

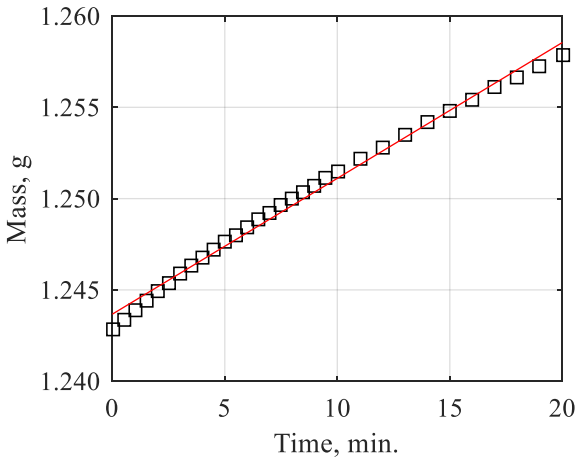

Figure 7: Mass of HIPEP sample over time at room temperature, atmospheric conditions.

Further, fresh samples of HIPEP as delivered from the manufacturer contain an unknown mass of moisture absorbed already (DSSP estimates 1-5%). To quantify this mass for the samples used in this work, three fresh, untested samples were inserted in the vacuum test facility for about 3 hours such that most of the water can be assumed to have evaporated. These samples were then removed from vacuum and their masses measured, while recording the time of this process. Using the absorption rate reported above, the mass in vacuum of the samples can be calculated, as well as the percentage of water content in the propellant. The details of these measurements and calculations are shown in Table III.

Table III: Water content measurements for samples of HIPEP.

Sample	Fresh Mass, g	Final Mass, g	Time to measurement, min.	Vacuum Mass, g	% Water
1	1.28055	1.23320	9.10	1.2264	3.70%
2	1.29476	1.24007	10.05	1.2325	4.22%
3	1.29233	1.24140	11.00	1.2332	3.94%

This experiment indicates that the HIPEP samples used in this work have a water content of about 4.0%. Additionally, in the process of venting the vacuum test facility and then measuring the mass of the sample, each sample gained, on average, about 1% total mass in water content. These values significantly skew the ablated mass per energy measurements presented in Table II, as mentioned in section IV-B. However, now that an estimate of the water content of the HIPEP samples at measurement has been obtained, the measurements in Table II can be corrected. Table IV shows the same measurements from Table II for PTFE, along with new values for HIPEP that have been adjusted for water content.

Table IV: Ablation mass measurements adjusted to account for HIPEP water content.

Propellant	Voltage, V	Mass Loss, mg	Pulses	Δm/Pulse, μg	Δm/Energy, μg/J
PTFE	2000	4.52	200	22.60	2.30
		2.95	150	19.67	2.00
		2.89	175	16.51	1.68
HIPEP	2000	1.68	75	22.46	2.28
		1.83	125	14.66	1.49
		6.19	130	47.60	4.84

Adjusting the values to account for the moisture content of the HIPEP drastically reduces the measured ablation mass per energy, though it introduces more variance. The average mass loss per pulse is now 28.24 μg. For the pulse energy of 9.84 J, this is 2.87 μg/J. This value is much closer to the value of 5.4 μg/J found in previous work with HIPEP. Additionally, the mass loss per energy is now closer to the measured mass loss of PTFE in pulsed plasma thrusters. The ablation mass loss is an important consideration in propellant usage efficiency in PPTs, and this information will be useful when considering HIPEP for use in a pulsed electric propulsion device.

V. Conclusion

A small scale arc discharge test article was operated with two propellants. The first was the often used PPT propellant, PTFE. The second was a novel electric solid propellant, which has been shown to exhibit similar behavior to PTFE when used as fuel in a PPT. For each propellant, the ablation mass loss and the electric current of the discharge were measured. The raw mass loss measurements indicated a mass loss per energy (specific ablation) of 31.7 μg/J for the electric solid propellant, HIPEP, which is much higher than the 1.99 μg/J measured for PTFE. However, the high moisture content of the hygroscopic HIPEP material was suspected to artificially inflate that number. A study of the water mass percentage of the propellant shows that the samples as received from the supplier are about 4.0% water by mass. It was also shown that the propellant absorbs moisture at a rate of 0.75 mg/min. at 101 kPa, 296 K and 50% relative humidity. When they are removed from the vacuum chamber after testing, each sample gains about 1% water by mass over the ~10 min. before it is weighed. By removing the estimated mass of water from the original measurements for specific ablation, a new estimate of 2.87 μg/J was obtained for HIPEP. The reduced specific ablation indicates a possible increase in propellant utilization efficiency for the given operating conditions over that of PTFE.

The current through the discharge circuit was measured during each pulse with a current transformer. This current was also modeled using an idealized inductance-capacitance-resistance model with constant elements. By matching the modeled current waveform to the measured one, an estimate for the circuit resistance and inductance was obtained. For the PTFE propellant, the resistance was estimated to be 165 mΩ and the inductance 764 nH. The resistance for the HIPEP circuit was estimated to be similar, about 159 mΩ but the inductance was estimated to be 458 nH. A change in inductance is unexpected, as the circuit and its geometry are identical between propellants. However, it is suspected that the presence of the electrically conductive and isolated HIPEP present between the high voltage electrodes affects the circuit inductance. Additionally, it was noted that the main capacitor was not fully discharged during testing with HIPEP. Specifically, the capacitor voltage before the discharge was 2000V and after the discharge it was typically about 1000V. For PTFE, the calculated energy dissipated by the discharge circuit was ~91% of the electrically stored energy but for HIPEP the energy dissipation was only 39% of the stored energy. This phenomenon warrants further investigation.

References

[1]Sawka, W. N., "Pulse Performance and Power Requirements for Electrically Controlled Solid Propellant," *54th JANNAF Propulsion Meeting*, JANNAF, Denver, CO, 2007.

[2]Sawka, W. N., Katzakian, A., and Grix, C., "Solid State Digital Cluster Thrusters for Small Satellites, Using High Performance Electrically Controlled Extinguishable Solid Propellants," *AIAA/USU Conference on Small Satellites*, AIAA, Logan, UT, 2005.

[3]Sawka, W. N., and McPherson, M., "Electrical Solid Propellants: A Safe, Micro to Macro Propulsion Technology," *49th AIAA/ASME/SAE/ASEE Joint Propulsion Conference*, AIAA, San Jose, CA, 2013. doi: 10.2514/6.2013-4168

[4]Burton, R. L., and Turchi, P. J., "Pulsed Plasma Thruster," *Journal of Propulsion and Power*, Vol. 14, No. 5, 1998, pp. 716-735. doi: 10.2514/2.5334

[5]Guman, W. J., and Nathanson, D. M., "Pulsed Plasma Microthruster Propulsion System for Synchronous Orbit Satellite," *Journal of Spacecraft and Rockets*, Vol. 7, No. 4, 1970, pp. 409-415. doi: 10.2514/3.29955

[6]LaRocca, A. V., "Pulsed Plasma Thruster System for Attitude and Station Control of Spacecraft," *First Western Space Congress*, 1970, pp. 688-702.

[7]Vondra, R. J., and Thomassen, K. I., "Flight Qualified Pulsed Electric Thruster for Satellite Control," *Journal of Spacecraft and Rockets*, Vol. 11, No. 9, 1974, pp. 613-617. doi: 10.2514/3.62141

[8]Gatsonis, N. A., Lu, Y., Blandino, J., Demetriou, M. A., and Paschalidis, N., "Micropulsed Plasma Thrusters for Attitude Control of a Low-Earth-Orbiting Cubesat," *Journal of Spacecraft and Rockets*, Vol. 53, No. 1, 2016, pp. 57-73. doi: 10.2514/1.A33345

[9]Rayburn, C. D., Campbell, M. E., and Mattick, A. T., "Pulsed Plasma Thruster System for Microsatellites," *Journal of Spacecraft and Rockets*, Vol. 42, No. 1, 2005, pp. 161-170. doi: 10.2514/1.15422

[10]Burton, R. L., Bushman, S. S., and Antonsen, E. L., "Arc Measurements and Performance Characteristics of a Coaxial Pulsed Plasma Thruster," *34th AIAA/ASME/SAE/ASEE Joint Propulsion Conference and Exhibit*, AIAA, Cleveland, OH, 1998. doi: 10.2514/6.1998-3660

[11]Wilson, M. J., Bushman, S. S., and Burton, R. L., "A Compact Thrust Stand for Pulsed Plasma Thrusters," *25th International Electric Propulsion Conference*, Cleveland, OH, 1997.

[12]Antonsen, E. L., Burton, R. L., Reed, G. A., and Spanjers, G. G., "Effects of Postpulse Surface Temperature on Micropulsed Plasma Thruster Operation," *Journal of Propulsion and Power*, Vol. 21, No. 5, 2005, pp. 877-883. doi: 10.2514/1.13032

[13]Gatsonis, N. A., Juric, D., Stechmann, D., and Byrne, L., "Numerical Analysis of Teflon Ablation in Pulsed Plasma Thrusters," *43rd AIAA/ASME/SAE/ASEE Joint Propulsion Conference & Exhibit*, AIAA, Cincinnati, OH, 2007. doi: 10.2514/6.2007-5227

[14]Keidar, M., Boyd, I. D., Antonsen, E. L., Gulczinski III, F. S., and Spanjers, G. G., "Propellant Charring in Pulsed Plasma Thrusters," *Journal of Propulsion and Power*, Vol. 20, No. 6, 2004, pp. 978-984. doi: 10.2514/1.2471

[15]Mikellides, P., and Turchi, P., "Modeling of Late-Time Ablation in Teflon Pulsed Plasma Thrusters," *32nd Joint Propulsion Conference and Exhibit*, AIAA, Lake Buena Vista, FL, 1996. doi: 10.2514/6.1996-2733

[16]Ruchti, C. B., and Niemeyer, L., "Ablation Controlled Arcs," *IEEE Transactions on Plasma Science*, Vol. PS-14, No. 4, 1986, pp. 423-434.

[17]Schönherr, T., Komurasaki, K., and Herdrich, G., "Propellant Utilization Efficiency in a Pulsed Plasma Thruster," *Journal of Propulsion and Power*, Vol. 29, No. 6, 2013, pp. 1478-1487. doi: 10.2514/1.B34789

[18]Seeger, M., Tepper, J., Christen, T., and Abrahamson, J., "Experimental Study on Ptfe Ablation in High Voltage Circuit-Breakers," *Journal of Physics D: Applied Physics*, Vol. 39, No. 23, 2006, pp. 5016-5024. doi: 10.1088/0022-3727/39/23/018

[19]Sigma-Aldrich, "Ionic Liquids for Electrochemical Applications," *Aldrich ChemFiles*, Vol. 5, No. 6, 2005.

[20]Jahn, R. G., *Physics of Electric Propulsion*, New York: McGraw-Hill, 1968.

[21]Shaw, P., "Pulsed Plasma Thrusters for Small Satellites." Vol. Ph. D., University of Surrey, 2011.

[22]Glascock, M. S., Rovey, J. L., Williams, S., and Thrasher, J., "Plasma Plume Characterization of Electric Solid Propellant Micro Pulsed Plasma Thrusters," *51st AIAA/SAE/ASEE Joint Propulsion Conference*, AIAA, Orlando, FL, 2015. doi: 10.2514/6.2015-4185

[23]Glascock, M. S., Rovey, J. L., Williams, S., and Thrasher, J., "Observation of Late-Time Ablation in Electric Solid Propellant Pulsed Microthrusters," *52nd AIAA/SAE/ASEE Joint Propulsion Conference*, AIAA, Salt Lake City, UT, 2016. doi: https://doi.org/10.2514/6.2016-4845

[24]Glascock, M. S., Rovey, J. L., Williams, S., and Thrasher, J., "Characterization of Electric Solid Propellant Pulsed Microthrusters," *Journal of Propulsion and Power*, (to be published).